

Communication

The Effect of a Weak Magnetic Field (0 T to 0.4 T) on the Valence Band and Intramolecular Hydrogen of Inorganic Aerosol Metal–Nitrogen Gas Chemical Reactions in a Sparking Discharge Process

Stefan Ručman ¹ , Chatdanai Boonruang ¹ and Pisith Singjai ^{1,2,*}

¹ Department of Physics and Materials Science, Faculty of Science, Chiang Mai University, Chiang Mai 50200, Thailand; stefan_rucman@cmu.ac.th (S.R.); chatdanai.b@cmu.ac.th (C.B.)

² Material Science Research Center, Faculty of Science, Chiang Mai University, Chiang Mai 50200, Thailand

* Correspondence: pisith.s@cmu.ac.th

Received: 13 November 2020; Accepted: 14 December 2020; Published: 17 December 2020



Abstract: The effects of a weak magnetic field on chemical reactions are still not well understood. In our research, we used a sparking discharge process to ionize and atomize different metal wires in ambient air under usual atmospheric conditions, with and without the presence of a magnetic field. Products were collected on a glass substrate and additionally characterized for the presence of nitrogen or nitride bonding with XPS. All samples sparked with no magnetic field provided an evidence of nitride formation. Additional characterization and comparison of samples prepared inside and outside a magnetic field was performed using FTIR and collected in deionized (DI) water to investigate the influence on conductivity and pH. When the magnetic field was present during sparking discharge, a higher concentration of nanoparticles was produced.

Keywords: sparking process; the magnetic field induced crystallization; chemical reactions in magnetic field; ambient crystallization; plasma processes

In 2018, we published a paper [1] on increasing the longevity of zerovalent iron nanoparticles (nZVI). In our research with a sparking discharge process, we applied a 0.4 Tesla magnetic field using a permanent magnet (Neodymium Magnet Physical Properties are graded according to information available on following website from K&J Magnetics, Inc., Pipersville, PA, USA, company, URL saved on web.archive.org <https://www.kjmagnetics.com/specs.asp>) to produce small and highly crystalline nano zerovalent iron (nZVI) particles. However, when we used a magnetic field of less than 0.4 T in strength, specifically in the range from 0.1 T to 0.3 T, we produced particles with different characteristics (see electronic supplementary information (ESI)) and their concentration was lower. The resulting aerosol concentrations were measured with a differential mobility analyzer (DMA) [2] at different magnetic field strengths. The results led us to investigate the reasons behind the measured influence of a weak magnetic force on chemical reactions and crystallization. The investigation focused on the abundance of free radicals and plasma ions produced during the sparking discharge process [3] and, therefore, the variety of singlet–triplet pairs which can, at certain discrete magnetic field strengths, prolong the radical pair crossing process. Furthermore, we focused on the influence of the magnetocrystalline anisotropy [4] on the lattice constant, which provided the preferred orientation, and was due to the spin-orbit coupling.

In the experimental research, we analyzed the products of a chemical reaction from a sparking discharge process, corresponding to the breaking voltage region of a current–voltage plasma discharge [5] curve (as represented and described in: Wagenaars, E. (2006). Plasma

breakdown of low-pressure gas discharges. Eindhoven: Technische Universiteit Eindhoven. <https://doi.org/10.6100/IR614696> and Bogaerts A, Neyts E, Gijbels R, Van der Mullen J. Gas discharge plasmas and their applications. *Spectrochimica Acta Part B: Atomic Spectroscopy*. 2002; 57(4), 609–58. See ESI for graphical representation). This synthesis method is also called spark ablation or spark explosion and approaches the nanoparticle synthesis via an aerosol-based chemical route [6–10]. Our research group approached a sparking process as a metal melt process [11–14] or as a metal vaporization with a high voltage for surface modification application. Nevertheless, both are based on the same physical mechanism, similar apparatuses (see ESI images) and the same processes or chemical reactions that take place in the sparking gap between the metal wires of sparking discharge apparatus. These processes, involving chemically active reactants, are represented in Figure 1. The anode and cathode are shown as simple metal wires that are the source of metal atoms. These wires (shown in ESI) were made from pure metal (metal wires of high purity were purchased from Advent Research Materials Ltd., Witney, UK) and were placed in electrode position of the sparking machine apparatus with a specific gap between their tips that prevented a short-circuit and to allow for the formation of breakdown voltage, a permanent discoid stacking magnet was placed below the sparking discharge and maintained at the same distance (3 mm) under all experimental conditions (0 T to 0.4 T) as is represented in the figure of graphical abstract.

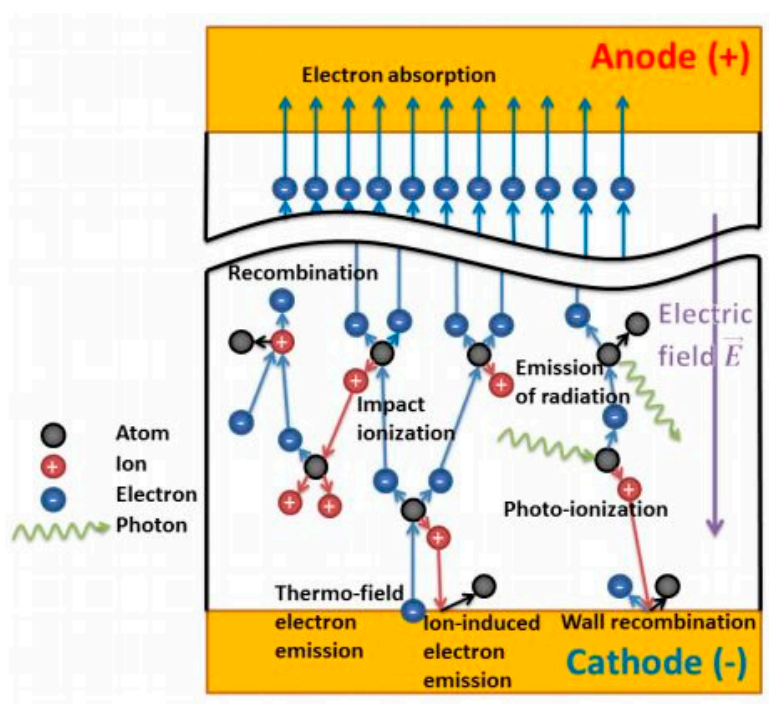


Figure 1. Schematics of the main processes involving electrons and ions which occur during spark discharge. From (Voloshko, 2015) (Image taken from: Andrey Voloshko. Nanoparticle formation by means of spark discharge at atmospheric pressure. *Plasma Physics* [physics.plasm-ph]. Université Jean Monnet—Saint-Etienne, 2015. English).

The magnetic field was generated from permanent discoid magnets that were stacked on top of each other in order to create different field strengths and was measured with a Phywe Tesla Meter calibrated and equipped with a hall probe; the sparking gap was distanced from the magnet equally in all conditions (0 T to 0.4 T). This is important because the gap consists of the air medium, which is a dielectric component made of atmospheric air (By using term atmospheric air we imply that it is non-dry air that contains 78% nitrogen, 21% oxygen, 0.93% argon, 0.04% carbon dioxide, and small amounts of other gases. Air also contains on average around 1% of water vapor.). In this gap, a nitrification reaction occurs between metal ions or metallic aerosols, which are melted or ablated at a high voltage

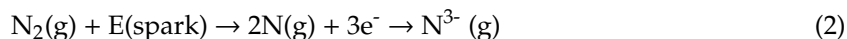
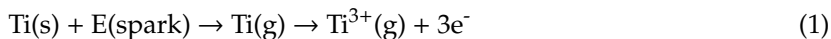
low current regime, and excite gas molecules of nitrogen [1,15] located in the dielectric medium in the gap. To summarize all reactions in the sparking gap; gasses can react between each other and/or with the vapor/aerosol of the metal wire. The latter consists of atomized metal, excited metal atoms, metal radicals, and charged aerosol particles. We characterized the surface composition, the products of the chemical reaction of sparking discharge and the nitrification with X-ray photoelectron spectroscopy (XPS). In our previous research, we have reported on iron and zinc metal wire sparking [1,2] and in the current research, investigated cobalt, nickel, titanium, vanadium, and tungsten. A full XPS report is available in ESI, and we only summarize N 1 s peak in Table 1 below. All aerosol nanoparticles produced by sparking discharge process were collected on a quartz substrate, beneath which was sometimes placed a permanent neodymium magnet, depending on the purpose of the experiment. The magnet strengths used were 0 T, 0.2 T and 0.4 T, and there was a clear influence on the crystalline structure of precipitated metal aerosols even at 0.4 T; however, we observed a metal nitride peak (400 eV to 398 eV) only when the magnetic field is less than 0.4 T.

Table 1. Comparative representation of N 1s peaks of different metal wires used in the sparking discharge process with no magnetic field under different atmosphere.

Metal Wire	Position (eV)	FWHM (eV)	Atomic Conc. (%)
Nickel–air	400.3/407.346	2.992	3.35
Nickel–pure N ₂	400.089/398.744	2.687	2.92
Cobalt–atmospheric air	407.304/399.806	1.421	-
Cobalt	407.191/400.211/399.155	2.370	1.02
Vanadium–air	407.228/401.873/400.032	2.875	5.08
Titanium	407.223/400.100	2.576	1.97
Vanadium	401.500	2.488	4.20
Tungsten	401.800	2.842	4.68

The quality assurance and reproducible results were achieved by sparking inside air, pure nitrogen, and in the presence or absence of a magnetic field. It is clear that the lack of observable N 1 s XPS peak was due to the interference of a magnetic force. In Table 1, we present the results of sparking several types of metal wires on substrates underneath which a permanent magnet or magnetic material was not placed, performed either under pure nitrogen or ambient air atmosphere. In our XPS results, we can observe peak metal nitride values at 399 eV and peak nitrites at 407 eV.

Sparked cobalt reacts directly with nitrogen gas to produce cobalt nitride which consists of Co³⁺ and N³⁻, which implies that the breakdown voltage of the sparking gap is sufficient to break the triple bond of the nitrogen molecule. Titanium and titanium nitride are known for their noble-like properties, and in this case, the chemical reaction in the sparking discharge gap follows these steps:



The chemical reactions from Formulas (1) and (2) combine in the sparking gap to precipitate titanium nitride. The process is represented in Formula 3.



Thermodynamically and kinetically, this reaction is possible [16,17]. The sparking process is a high energy nanomaterial generation process that allows for the vaporization/aerosolization of metals. Nitrogen molecules in the sparking gap are excited by the discharge energy flowing from the tips of the wires that are subsequently ionized. This leads to breakdown of the nitrogen triple bond. What follows is the atomization of metal wires which provides a high surface-area-to-volume ratio for the reaction

to take place [18–20]. Moving away from the chemical reaction process, we need to prove why the described process of nitrification does not occur at a magnetic field of 0.4 Tesla and above.

We have previously published XRD and SAED data (Selected area electron diffraction) of sparked iron wire at 0 T to 0.4 T, in a pure nitrogen environment [1], as well as of sparked zinc in a pure carbon dioxide (CO₂) and nitrogen atmosphere using the same magnetic field strengths [2]. In Table 2, we summarize those findings, including the data of sparking metal wires in atmospheric conditions using an external magnetic field [11].

Table 2. Comparison of Miller indices of different metal wires used as sparking material, as published [1,2,11].

Metal	Conditions	Miller Indices	Crystallographic Reference
Iron (Fe)	0 T, pure N ₂	(002,211) and (111)	73-2102 and 83-087726
Iron (Fe)	0.2 T, pure N ₂	(111,200,220) and (110)	04-016-4995; 01-080-3816
Iron (Fe)	0.4 T, pure N ₂	(110)	98-000-0259
Zinc (Zn)	0.2 T and 0.4 T, pure N ₂	(100) (212) (400)	00-005-0664; 00-023-0740; 00-035-0762
Tungsten (W)	0.4 T, ambient air	(112) (211)	00-041-1230; 03-065-6453
Nickel	0.4 T, ambient air	(111) and (200); (200)	03-065-2865 01-083-8042
Copper	0.4 T, ambient air	(002) (11-1); (111) (200)	01-080-0076. 03-065-9743
Indium (In)	0.4 T, ambient air	(101) (002) (110); (222)	03-065-9292, 01-071-2194

These Miller indices appear in XRD when sparked inside of a magnetic field with no thermal annealing or any subsequent treatment that could increase the crystallinity. A higher magnetic field, higher crystallinity, and a smaller number of peaks will appear. However, as stated previously, atmospheric metal nitride formation will only occur if the magnetic field beneath the substrate where precipitate is collected is less than 0.4 T. At any amount of magnetic field, the particles will assume a preferred orientation, which is a well-known texturing of a magnetic field [21,22]. This influence on the size and structure of a crystal can be explained by the fluctuation in energy; however, energy fluctuation cannot explain different chemical products, so a further examination of cohesive energy is required.

In terms of synthesis of new compounds and in terms of solid reaction, it is especially convenient to use cohesion energy because it signifies the energy required for solids to assemble the atoms into a structural array of reacting free atoms or reactants. The sparking discharge process disassembles solids (vaporizes) and the external magnetic field stabilizes them in a way that affects the binding of atoms

These results explain why we see nitrides at 0.2T with zinc [2] and iron [1], but do not detect them with XPS at magnetic fields equal to or higher than 0.4 T. Based on these results, we conclude with a universal chemical equation for the metal nitrides of transition elements in chemical reactions that are happening inside an external magnetic field of 0.2 T and 0.4 T, under ambient air conditions.



The second important experimental observation of materials prepared in weak magnetic fields is that those prepared by sparking inside of the magnetic field are bound together strongly and have good mechanical strength. These nanoparticles are produced by a sparking discharge process [11], and if we introduce a magnetic field in the sparking gap, we will produce nanostructures with resistivity to corrosion and humidity in comparison with those which are not prepared inside a magnetic field, which are amorphous and prone to fast corrosion. Previously, we have shown influence of a uniform magnetic field on the concentration of cobalt at sparked nickel wires [23], which led us to believe that intramolecular bonding, that plays important part in the cohesiveness of material, can be characterized to evaluate for their presence inside and outside of magnetic field. FTIR experiments were conducted. Nanoparticles generated from sparking machines were collected on a quartz surface, under which was placed a 0.4 T permanent magnet. Results are shown in Figure 2, and there is an indication that the composition of thin films prepared in the magnetic field lacks metal chelate complexes and intramolecular hydrogen bonds.

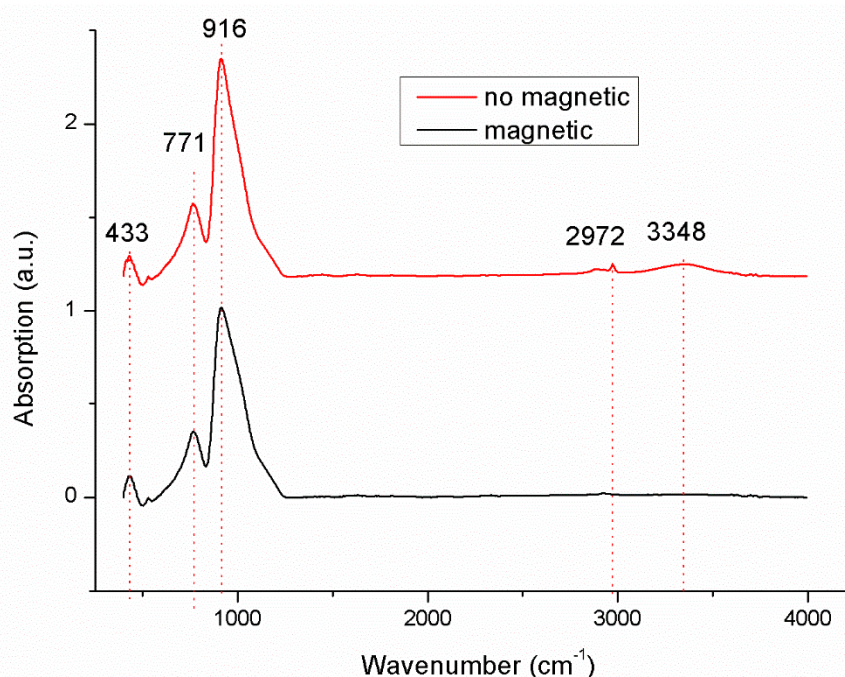


Figure 2. FTIR spectra of sparked discharged wires inside and outside of magnetic field.

The absence of FTIR spectra band positions at 2972 cm^{-1} and 3348 cm^{-1} in the results on the samples prepared inside of a magnetic field represent important parameters in explaining the role of cohesive forces. Namely, absence of these functional groups represents the absence of intermolecular bonding for synthetic materials prepared inside of a weak magnetic field.

It is important to note that sparking in a magnetic field also influences the valence band of sparking discharge deposited nanoparticles, as represented in Figure 3.

The valence band spectra of XPS are important for providing information about solid systems [24]. Due to the integration of different kinds of elements in the nanomaterials prepared inside and outside of the magnetic field, we can therefore synthesize materials with lower binding energies of their core electrons [25] if materials are prepared inside of a magnetic field.

To further investigate the effects of magnetic fields on spark discharge, represented in Figure 4, we placed deionized (DI) water below the sparking head and monitored differences in pH and conductivity, with and without a magnetic field present during the sparking discharge process.

The collection of nanoparticles in DI water and measuring of the parameters is represented in Table 3. Observed are the trends in effects of conductivity with increases if a magnetic field is present,

which is due to the higher concentration of particles produced from a sparking head when a magnetic field is present, and the lowering of pH is due to radical production from plasma created in discharge.

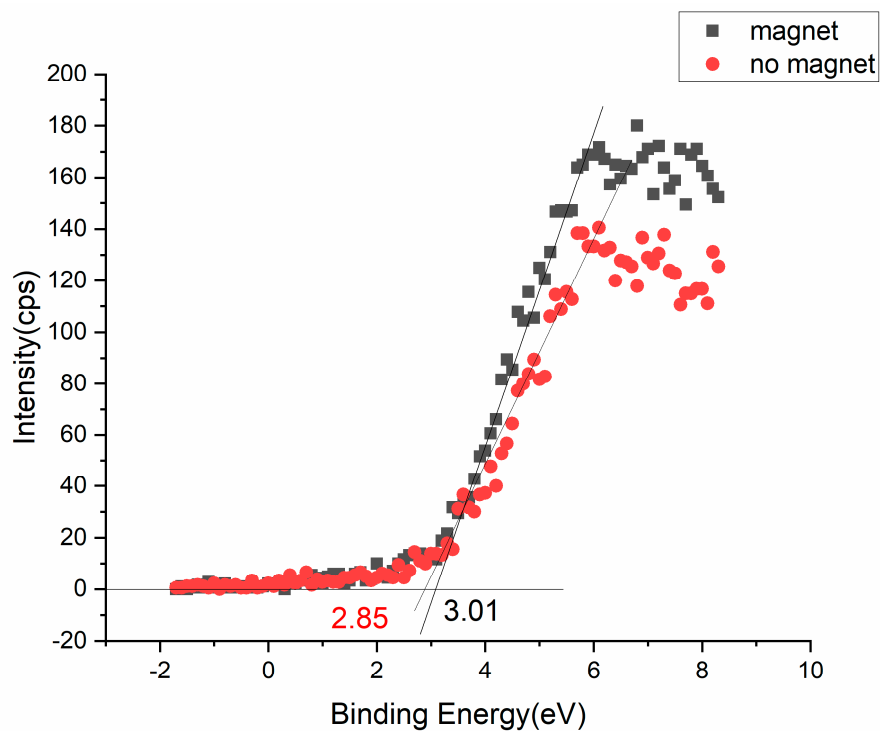


Figure 3. XPS binding energy of nanoparticles collected with sparking discharge. Same sample as for FTIR.

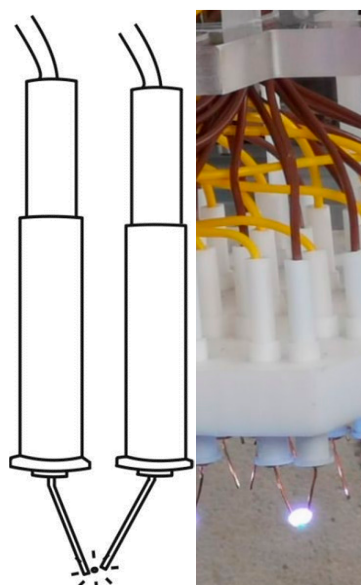


Figure 4. Sparking discharge head, with wires that discharged a high voltage low current, and particles/radical collected in deionized (DI) water.

Drops in pH can be attributed to the formation of acid-like rain phenomena in sparking discharge, and magnetic field does not influence this reaction; however due to increases in the number of particles produced while a magnetic field is present, there is an increase in conductivity.

Table 3. DI water parameters of sparking aluminium wires.

Time	Spark Energy	Temperature (°C)	pH	Conductivity (µS/cm) No Mag. Field	Conductivity (µS/cm) Mag. Field
0 min	0 kV 0 mA	28	7	1.35	0.68
5 min	4.75 kV 0.61 mA; 4.40 kV 0.55 mA;	28	6.38	6.17	13.08
15 min	4.78 0.57; 4.42 0.57;	28	6.18	15.93	27.70
30 min	4.76 0.58; 4.42 0.53;	28	5.77	29.68	34.84
45 min	4.77 0.58; 4.42 0.55	28	5.46	39.7	49.9
60 min	4.85 0.60; 4.48 0.54;	27	4.90	48.8	59.4
75 min	4.9 0.6; 4.48 0.55	27	4.58	68.1	79.1

We investigated the influence of applying a weak magnetic field (0.1 T to 0.4 T) during a sparking discharge reaction of transition metals (Fe, Ni, V, Ti, W, Co, Zn) and dielectric or insulating gasses (N₂, CO₂, O₂). In this paper, we provide experimental evidence of nitride formation influenced by the application of a weak external magnetic field influence on the valence band as well as the concentration of aerosol produces. This paper sheds light on an important aspect of chemical reactions in magnetic fields, which further develops the overall understanding. Chemical bonding characterization was performed using X-ray photoelectron spectroscopy (XPS) and Fourier-transform infrared spectroscopy (FTIR). Results also showed an effect on pH, intermolecular hydrogen, and the number of particles produced from sparking discharge.

Supplementary Materials: The following are available online at <http://www.mdpi.com/2073-4352/10/12/1141/s1>.

Author Contributions: Conceptualization, S.R. and P.S.; methodology, S.R.; software, C.B.; validation, S.R., C.B.; formal analysis, S.R. and P.S.; investigation, S.R.; data curation, P.S. and C.B.; writing—original draft preparation, S.R.; writing—review and editing, S.R.; visualization, C.B.; supervision, P.S. and S.R.; project administration, S.R.; funding acquisition, S.R. and P.S. All authors have read and agreed to the published version of the manuscript.

Funding: This research received Chiang Mai University Funding.

Acknowledgments: Stefan Ručman would like to thank the postdoctoral fellowship from Chiang Mai University for help and support.

Conflicts of Interest: The authors declare no conflict of interest.

References

1. Stefan, R.; Jakmunee, J.; Punyodom, W.; Singjai, P. A novel strategy for longevity prolongation of iron-based nanoparticle thin films by applied magnetic force. *New J. Chem.* **2018**, *42*, 4807.
2. Ručman, S.; Intra, P.; Kantarak, E.; Sroila, W.; Kumpika, T.; Jakmunee, J.; Punyodom, W.; Arsić, B.; Singjai, P. Influence of the magnetic field on bandgap and chemical composition of zinc thin films prepared by sparking discharge process. *Sci. Rep.* **2020**, *10*, 1.
3. Aleksandrov, N.L.; Bazelyan, E. M Ionization processes in spark discharge plasmas. *Plasma Sources Sci. Technol.* **1999**, *8*, 285. [[CrossRef](#)]
4. Kumar, S.; Supriya, S.; Pandey, R.; Pradhan, L.K.; Singh, R.K.; Kar, M. Effect of lattice strain on structural and magnetic properties of Ca substituted barium hexaferrite. *J. Magn. Magn. Mater.* **2018**, *458*, 30. [[CrossRef](#)]
5. Ghaleb, F. Belasri, A Numerical and theoretical calculation of breakdown voltage in the electrical discharge for rare gases. *Radiat. Eff. Defects Solids* **2012**, *167*, 377. [[CrossRef](#)]

6. Kohut, A.; Ludvigsson, L.; Mueller, B.O.; Deppert, K.; Messing, M.E.; Galbács, G.; Geretovszky, Z. From plasma to nanoparticles: Optical and particle emission of a spark discharge generator. *Nanotechnology* **2017**, *28*, 475603. [[CrossRef](#)]
7. Kohut, A.; Galbács, G.; Márton, Z.; Geretovszky, Z. Characterization of a copper spark discharge plasma in argon atmosphere used for nanoparticle generation. *Plasma Sources Sci. Technol.* **2017**, *26*, 045001. [[CrossRef](#)]
8. Kohut, A.; Villy, L.P.; Ajtai, T.; Geretovszky, Z.; Galbács, G. The effect of circuit resistance on the particle output of a spark discharge nanoparticle generator. *J. Aerosol Sci.* **2018**, *118*, 59. [[CrossRef](#)]
9. Tabrizi, N.S.; Xu, Q.; Van Der Pers, N.M.; Schmidt-Ott, A. Generation of mixed metallic nanoparticles from immiscible metals by spark discharge. *J. Nanoparticle Res.* **2010**, *12*, 247. [[CrossRef](#)]
10. Tabrizi, N.S.; Ullmann, M.; Vons, V.A.; Lafont, U.; Schmidt-Ott, A. Generation of nanoparticles by spark discharge. *J. Nanoparticle Res.* **2009**, *11*, 315. [[CrossRef](#)]
11. Ručman, S.S.; Panyodom, W.; Jakmune, J.; Singjai, P. Inducing Crystallinity of Metal Thin Films with Weak Magnetic Fields without Thermal Annealing. *Crystals* **2018**, *8*, 362. [[CrossRef](#)]
12. Thongpan, W.; Louloudakis, D.; Pooseekheaw, P.; Kumpika, T.; Kantarak, E.; Panthawan, A.; Thongsuwan, W.; Singjai, P. Porous CuWO₄/WO₃ composite films with improved electrochromic properties prepared by sparking method. *Mater. Lett.* **2019**, *257*, 126747. [[CrossRef](#)]
13. Hankhantod, A.; Kantarak, E.; Sroila, W.; Kumpika, T.; Singjai, P.; Thongsuwan, W. α -Fe₂O₃ modified TiO₂ nanoparticulate films prepared by sparking off Fe electroplated Ti tips. *Appl. Surf. Sci.* **2019**, *477*, 116. [[CrossRef](#)]
14. Kumpika, T.; Thongsuwan, W.; Singjai, P. Optical and electrical properties of ZnO nanoparticle thin films deposited on quartz by sparking process. *Thin Solid Film.* **2008**, *516*, 5640. [[CrossRef](#)]
15. Quintero, J.; Mariño, A.; Šiller, L.; Restrepo-Parra, E.; Caro-Lopera, F. Rocking Curves of Gold Nitride Species Prepared by Arc Pulsed - Physical Assisted Plasma Vapor Deposition. *Surf. Coat. Technol.* **2017**, *309*, 249. [[CrossRef](#)]
16. Seki, I.; Yamaura, S.I. Reduction of Titanium Dioxide to Metallic Titanium by Nitridization and Thermal Decomposition. *Mater. Trans.* **2017**, *58*, 361. [[CrossRef](#)]
17. Vahlas, C.; Ladouce, B.D.; Chevalier, P.Y.; Bernard, C.; Vandenbulcke, L. A thermodynamic evaluation of the Ti-N system. *Thermochim. Acta* **1991**, *180*, 23. [[CrossRef](#)]
18. Kim, W.Y.; Jo, J.O.; Chung, T.I.; Kim, D.S.; Pak, J.J. Thermodynamics of Titanium, Nitrogen and TiN Formation in Liquid Iron. *ISIJ Int.* **2007**, *47*, 1082. [[CrossRef](#)]
19. Jones, F.L. Electrode Erosion by Spark Discharges. *Br. J. Appl. Phys.* **1950**, *1*, 60. [[CrossRef](#)]
20. Cundall, C.M.; Craggs, J.D. Electrode vapour jets in spark discharges. *Spectrochim. Acta* **1955**, *7*, 149. [[CrossRef](#)]
21. De Rango, P.; Lees, M.; Lejay, P.; Sulpice, A.; Tournier, R.; Ingold, M.; Germi, P.; Pernet, M. Texturing of magnetic materials at high temperature by solidification in a magnetic field. *Nature* **1991**, *349*, 770. [[CrossRef](#)]
22. Masahashi, N.; Matsuo, M.; Watanabe, K. Development of preferred orientation in annealing of Fe-3.25%Si in a high magnetic field. *J. Mater. Res.* **1998**, *13*, 457. [[CrossRef](#)]
23. Tippo, P.; Thongsuwan, W.; Wiranwetchayan, O.; Kumpika, T.; Kantarak, E.; Singjai, P. Influence of Co concentration on properties of NiO film by sparking under uniform magnetic field. *Sci. Rep.* **2020**, *10*, 15690. [[CrossRef](#)] [[PubMed](#)]
24. Foix, D.; Martinez, H.; Pradel, A.; Ribes, M.; Gonbeau, D. XPS valence band spectra and theoretical calculations for investigations on thiogermanate and thiosilicate glasses. *Chem. Phys.* **2006**, *323*, 606–616. [[CrossRef](#)]
25. Morita, A. Theory of Cohesive Energies and Energy-Band Structures of Diamond-Type Valence Crystals: The Method of SLCO, II. *Prog. Theor. Phys.* **1958**, *19*, 534–540. [[CrossRef](#)]

Publisher's Note: MDPI stays neutral with regard to jurisdictional claims in published maps and institutional affiliations.



© 2020 by the authors. Licensee MDPI, Basel, Switzerland. This article is an open access article distributed under the terms and conditions of the Creative Commons Attribution (CC BY) license (<http://creativecommons.org/licenses/by/4.0/>).